Spatial-temporal distribution of deoxynivalenol, aflatoxin B1, and zearalenone in the solid-state fermentation basin of traditional vinegar and their potential correlation with microorganisms

Food Chemistry

Spatial-temporal distribution of deoxynivalenol, aflatoxin B1, and zearalenone in the solid-state fermentation basin of traditional vinegar and their potential correlation with microorganisms

--Manuscript Draft--

Manuscript Number:	FOODCHEM-D-23-01908R1
Article Type:	Research Article (max 7,500 words)
Keywords:	Mycotoxin; Chinese vinegar; Solid-state fermentation; Lactobacillus; Aspergillus
Corresponding Author:	Di Zhang CHINA
First Author:	Lingqin Shen
Order of Authors:	Lingqin Shen
	Yifan Wang
	Xin Li
	Ziqing Hou
	Jin Mao
	Jiyong Shi
	Maurizio Battino
	Michael N. Routledge
	Yunyun Gong
	Xiaobo Zou
	Di Zhang
Abstract:	This study revealed the spatial-temporal distribution of deoxynivalenol (DON), aflatoxin B1 (AFB1), and zearalenone (ZEN) during the acetic acid fermentation (AAF) of aromatic vinegar and the corresponding correlation with the microbial community. A total of 324 samples were collected during the AAF process to analyze the mycotoxin content. The average DON content fluctuated during the first 7 d, while the average AFB1 and ZEN levels increased at 5-7 d and 7-11 d, respectively, remaining stable until the end of fermentation. In addition, the significant AFB1 and ZEN content variation was limited to the cross-sectional sampling planes in the fermentation basin, while DON was heterogeneously distributed on the cross-sectional, horizontal, and vertical sampling planes. Furthermore, the redundancy analysis and Spearman correlation coefficients revealed close relationships between three mycotoxins and certain bacterial and fungal species. This study provides new information regarding the mycotoxins during solid-state fermentation of traditional vinegar.
Suggested Reviewers:	Zheng-Hong Xu Jiangnan University zhenghxu@jiangnan.edu.cn
	Vicente Sanchis University of Lleida vicente.sanchis@udl.cat
	Min Wang Tianjin University of Science and Technology minw@tust.edu.cn

Cover Letter

Dear Editor,

Thank you very much for your kind suggestions and the reviewers' comments. The manuscript entitled "***Spatial-temporal distribution of deoxynivalenol, aflatoxin B_1, and zearalenone in the solid-state fermentation basin of traditional vinegar and their potential correlation with microorganisms***" has been revised according to reviewers' comments. The itemized response to each reviewer's comments is attached. We hope that the revision is acceptable, and we look forward to hearing from you soon.

Sincerely yours,

Dr. / Prof. Di Zhang
School of Food and Biological Engineering,
Jiangsu University, Zhenjiang 212013, China
E-mail: d.zhang@ujs.edu.cn
Fax: +86 511 88780201

Spatial-temporal distribution of deoxynivalenol, aflatoxin B_1, and zearalenone in the solid-state fermentation basin of traditional vinegar and their potential correlation with microorganisms

Lingqin Shen[1]; Yifan Wang[1]; Xin Li[2]; Ziqing Hou[2]; Jin Mao[3]; Jiyong Shi[2]; Maurizio Battino[2,4,5]; Michael N. Routledge[2, 6] Yunyun Gong[7]; Xiaobo Zou[2]; Di Zhang[2]*

1. School of Chemistry and Chemical Engineering, Jiangsu University, Zhenjiang, 212013, China

2. School of Food and Biological Engineering, Jiangsu University, Zhenjiang, 212013, China

3. National Reference Laboratory for Agricultural Testing, Key Laboratory of Detection for Mycotoxins, Laboratory of Quality & Safety Risk Assessment for Oilseed Products (Wuhan), Ministry of Agriculture, Oil Crops Research Institute, Chinese Academy of Agricultural Sciences, Wuhan, 430062, China

4. International Research Center for Food Nutrition and Safety, Jiangsu University, Zhenjiang 212013, China

5. Department of Clinical Sciences, Faculty of Medicine, Polytechnic University of Marche, Ancona, Italy

6. Leicester Medical School, University of Leicester, Leicester, UK

7. School of Food Science and Nutrition, University of Leeds, Leeds, UK

*Corresponding author, d.zhang@ujs.edu.cn (Di Zhang)

ABSTRACT

This study revealed the spatial-temporal distribution of deoxynivalenol (DON), aflatoxin B_1 (AFB_1), and zearalenone (ZEN) during the acetic acid fermentation (AAF) of aromatic vinegar and the corresponding correlation with the microbial community. A total of 324 samples were collected during the AAF process to analyze the mycotoxin content. The average DON content fluctuated during the first 7 d, while the average AFB_1 and ZEN levels increased at 5-7 d and 7-11 d, respectively, remaining stable until the end of fermentation. In addition, the significant AFB_1 and ZEN content variation was limited to the cross-sectional sampling planes in the fermentation basin, while DON was heterogeneously distributed on the cross-sectional, horizontal, and vertical sampling planes. Furthermore, the redundancy analysis and Spearman correlation coefficients revealed close relationships between three mycotoxins and certain bacterial and fungal species. This study provides new information regarding the mycotoxins during solid-state fermentation of traditional vinegar.

Keywords

Mycotoxin; Chinese vinegar; Solid-state fermentation; *Lactobacillus*; *Aspergillus*

1 Introduction

East Asian countries have used solid-state fermentation for thousands of years to prepare beverages and condiments (Lu et al., 2018; Sun et al., 2022). This method is commonly used in China to produce soy sauce, Chinese vinegar, and Chinese liquor (Baijiu) (Liu et al., 2022 (1); Tu et al., 2022), with an annual total production of over 20 million tons (Shen, 2022).

Despite the widespread consumption of solid-state fermented food, consumer concern has increased regarding the quality and safety of these products (Zhang et al., 2022; Di et al., 2023). Due to raw material and substrate contamination and the vulnerability of the open fermentation environment to toxigenic fungal growth, solid-state fermented food is highly susceptible to mycotoxins (Liu et al., 2022 (2); Li et al., 2023). Recent evidence has revealed the presence of mycotoxins in final solid-state fermentation products such as soy sauce, horse bean-chili-paste, Korean soybean paste, and Baijiu (Lu et al., 2021; Jeong et al., 2019; Woo et al., 2019; Zhu et al., 2016). Fermented food contamination by mycotoxins poses a significant threat to public health since some are known or suspected carcinogens (Awuchi et al., 2022; Ekwomadu et al., 2021). Therefore, tracking mycotoxin occurrence and distribution during solid-state fermentation is essential.

Traditional Chinese vinegar is mostly produced using a typical aerobic solid-state fermentation technique. At least 14 main types are commercially available, including Zhenjiang aromatic vinegar (ZAV), Shanxi old mature vinegar, Fujian

Monascus vinegar, and Sichuan bran vinegar (Li et al., 2023).

Like most solid-state fermented food, the production of Chinese vinegar is complex. During ZAV production, the acetic acid fermentation (AAF) stage lasts 18 d and is regarded as the most important step due to acetic acid formation and flavor development (Wang et al., 2015). Typical AAF uses wheat bran and rice husk as solid-state fermentation substrates (vinegar Pei), which are mixed with vinegar seeds and alcoholic fermentation broth (Al-Dalali et al., 2023). This process also employs deep-bed concrete basin systems for intermittent vinegar Pei stirring and mixing (Huang et al., 2022). Although several studies have focused on the impact of fermentation processing on bioactive components and microbial community diversity during Chinese vinegar production (Gong et al., 2021; Yu et al., 2022), minimal research is available regarding the risk evaluation of mycotoxins in these products.

This study employs a ZAV model system involving the pilot production of a traditional Chinese vinegar to illuminate the spatial distribution of the primary mycotoxins during AAF and reveal the dynamic changes in the bacterial and fungal community compositions at different spatial locations in the fermentation basin. The correlation between the mycotoxin and microorganism diversity is analyzed to determine the potential microbial effect on the mycotoxin distribution during solid-state Chinese vinegar fermentation. This study is the first to characterize the mycotoxin levels and distribution variation during solid-state Chinese vinegar fermentation. The findings can help understand the factors causing mycotoxin

contamination in the solid-state fermentation substrate.

2 Materials and methods

2.1 Reagents and chemicals

The mycotoxin standards (deoxynivalenol (DON), zearalenone (ZEN), and aflatoxin B1 (AFB_1)) were obtained from Sigma-Aldrich (St. Louis, Mo, USA). The mycotoxin standard stock solution (100 mg/L for DON and ZEN and 10 mg/L for AFB_1) was prepared using methanol and stored at -80 °C until further use. HPLC grade methanol and acetonitrile were obtained from the Tianjin Concord Tech Reagent Company (Tianjin, China), while the pure water was prepared using a Milli-Q Water Purification System (Millipore Corporation, Billerica, MA, USA). The other chemicals and solvents were all analytically pure and purchased from Sinopharm Chemical Reagent Co. Ltd. (Shanghai, China). The immunoaffinity columns (WSKC04A, WSKC02B, and WSKC03A) for the targeted isolation of DON, AFB_1, and ZEN were purchased from Wisherkon Co. Ltd. (Wuhan, China).

2.2 The solid-state vinegar fermentation process

The traditional method was used for the ZAV solid-state fermentation process, consisting primarily of four stages: (I) starch saccharification, (II) alcohol fermentation, (III) AAF, and (IV) sealed fermentation. Stage III (i.e., AAF) was initiated by adding fermented rice mash obtained during stage II and seed Pei from the last AAF batch to the fermentation substrate (rice husk and wheat bran) (Shen et al., 2016).

According to the traditional technique, the AAF was performed in a fermentation basin using about 960 kg rice husk, 2550 kg wheat bran, 900 kg seed Pei, and fermenter rice mash. During the early AAF stage (1 d to 6 d), vinegar Pei was turned in increasing layers of 5 cm to 10 cm per day. During the first 3 d of AAF, the top vinegar Pei layer was covered with rice husk to preserve heat after each turning. From 4 d to 6 d, wheat bran was added to the vinegar Pei after turning, and the Pei was covered with rice husk again. The gradual increase in the turning depth allowed all the vinegar Pei layers to be turned over by the middle fermentation stage (7 d). During the final fermentation stage (8 d to 17 d), the vinegar Pei was thoroughly turned over daily.

2.3 Vinegar Pei sample collection

The vinegar Pei collection method is illustrated in Fig. 1. The fermentation basin (length × width × depth = 10 × 1.5 × 0.8 m) was selected as the sample collection area, where a total of 36 sampling points were established, which were distributed on 10 planes to enhance the mycotoxin distribution evaluation in different directions. Here, a_1, a_2, a_3, and a_4 represented cross-sectional planes divided in the x-axis direction, while b_1, b_2, and b_3 denoted the horizontal planes divided in the y-axis direction, and c_1, c_2, and c_3 signified the vertical planes divided in the z-axis direction. The vinegar Pei was sampled in the fermentation basin at 1 d, 3 d, 5 d, 7 d, 9 d, 11 d, 13 d, 15 d, and 17 d of the AAF process, obtaining 324 specimens.

To accurately describe the mycotoxin distribution and microorganisms during the

AAF process, the vinegar Pei samples were collected at the same points in three different fermentation basins on the same day, mixed thoroughly, and reduced via repeated coning and quartering (Yu et al., 2022). Here, 500 g of each vinegar Pei sample was sealed in sterile plastic bags and stored at -80 °C for further analysis. In addition, the Maiqu (the starter for the alcohol fermentation process), raw materials (rice husk and wheat bran), and final vinegar products were also collected.

2.4 The measurement of the moisture content and pH

The moisture level was determined using the gravimetric method (Li et al., 2012) by drying the vinegar Pei samples at 105 °C for 4 h. The moisture content was calculated using the following formula:

$$M = \frac{m_1 - m_2}{m_1} \times 100\%$$

where M is the moisture content (%), m_1 is the original vinegar Pei weight (g), and m_2 is the dehydrated vinegar Pei weight (g).

The pH of the vinegar Pei was determined according to a method delineated by Huang, et al. (2022). Here, a 10 g vinegar Pei sample was soaked with 30 mL water and agitated at 100 rpm for 3 h at 25 °C using a shaker, after which the supernatant was collected via centrifugation at 6000 rpm for 10 min. The pH was measured using a pH meter (pH.3B, Shanghai, China).

2.5 The quantification of three mycotoxins in the vinegar Pei via HPLC

2.5.1 DON extraction from the vinegar Pei

The DON was extracted from the vinegar Pei using a method described by Wall-

144 Martínez, et al. (2020) with slight modifications. A 25 g vinegar Pei sample was
145 mixed with 5 g of polyethylene glycol and extracted via ultrasonication with 100 mL
146 water in a clean ultrasonic bath for 30 min at 25 °C, after which the supernatant was
147 collected after centrifugation at 6000 rpm for 10 min. Next, 7.5 mL of the neutral
148 supernatant, 30 mL of phosphate buffered solution (PBS), and 3 mL eluent (methanol)
149 were passed separately through the immunoaffinity column at 1.5 mL/min, after
150 which 2 mL of DON extract was collected. The DON extract was evaporated in a
151 nitrogen stream (45 °C) and resuspended in 1.5 mL of water.

152 *2.5.2 AFB_1 extraction from the vinegar Pei*

153 The AFB_1 was extracted from the vinegar Pei using a method delineated by
154 Kong, et al. (2014) with slight modifications. A 25 g vinegar Pei sample was mixed
155 with 4 g of NaCl and extracted via ultrasonication with 70% MeOH (100 mL;
156 methanol:water = 70:30, v:v) in a clean ultrasonic bath for 30 min. Then, 10 mL of
157 supernatant was collected after centrifugation at 6000 rpm for 10 min and diluted with
158 30 mL of water. Next, 40 mL of the neutral supernatant, 30 mL of PBS, and 2 mL
159 eluent were passed separately through the immunoaffinity column at 1.5 mL/min,
160 after which 1 mL of AFB_1 extract was collected.

161 *2.5.3 ZEN extraction from the vinegar Pei*

162 The ZEN was extracted from the vinegar Pei using a technique described by
163 Wall-Martínez, et al. (2020). A 25 g vinegar Pei was mixed with 4 g of NaCl and
164 extracted via ultrasonication with 90% acetonitrile (ACN) (100 mL; ACN:water =

90:10, *v:v*) in a clean ultrasonic bath (30 min). Then, 10 mL of supernatant was collected via centrifugation (6000 rpm, 10 min) and diluted with 40 mL of water. Next, 50 mL of the neutral supernatant, 30 mL of PBS, and 2 mL eluent were passed through the immunoaffinity column (1.5 mL/min), respectively, after which 1 mL of ZEN extract was collected.

2.5.4 HPLC system

The DON was quantified using a Shimadzu LC-20AT HPLC system coupled with an SPD-220AV ultraviolet detector (Shimadzu, Kyoto, Japan). An HP-C18 column (250 mm × 4.6 mm, 5 μm particle size, Sepax Technologies, Inc, USA) was used for separation. The HPLC conditions were modified according to a method delineated by Wall-Martinez, et al. (2019). The mobile phase consisted of 20% MeOH (methanol:water = 20:80, *v:v*) and was pumped at a 0.8 mL/min flow rate. The chromatographic analysis was performed at 35 °C at an absorption wavelength of 218 nm.

In addition, the AFB_1 and ZEN were quantified using a Shimadzu LC-20AT HPLC system equipped with an RF-10AXL fluorescence detector (Shimadzu, Kyoto, Japan). The AFB_1 was measured using a mobile phase consisting of 65% ACN (ACN:water = 65:35, *v:v*), pumped at a flow rate of 0.8 mL/min. The chromatographic analysis was performed at 25 °C, while the AFB_1 was detected at an excitation wavelength of 360 nm and an emission wavelength of 440 nm (Chien, et al., 2018).

The ZEN was quantified using a mobile phase consisting of 60% MeOH (methanol:water = 60:40, *v:v*), pumped at a flow rate of 0.8 mL/min. The chromatographic analysis was performed at 40 °C, and the ZEN was detected at 274 nm (excitation) and 440 (emission) (Wall-Martinez et al., 2019), respectively.

The extracted samples were passed through a 0.22 μm filter before injecting 50 μL into the HPLC system. The calibration curve was established using five concentration levels for each mycotoxin (100 μg/kg, 200 μg/kg, 500 μg/kg, 1000 μg/kg, and 1500 μg/kg for DON, 0.25 μg/kg, 0.5 μg/kg, 1 μg/kg, 2 μg/kg, and 5 μg/kg for AFB_1, and 10 μg/kg, 20 μg/kg, 40 μg/kg, 80 μg/kg, and 150 μg/kg for ZEN). The regression equations between the concentration (x) and the peak area (y) of DON, AFB_1, and ZEN were $y = 91.33 \times x + 779.53$ with an R^2 of 0.9995 (Fig. S1), $y = 7532.15 \times x - 289.26$ with an R^2 of 0.9995 (Fig. S2), and $y = 273.31 \times x - 545.14$ with an R^2 of 0.9994 (Fig. S3), respectively. The DON, AFB_1, and ZEN retention times were 16.28 min, 6.08 min, and 14.76 min.

2.6 Microbial community analysis

The bacterial and fungal community structures in the raw material and vinegar Pei samples were analyzed via 16S rDNA and internal transcribed spacer (ITS) to determine the microbial communities during fermentation. The vinegar Pei samples for the microbiological analysis were collected from 10 sampling sites (at 2, 4, 5, 6, and 8 sampling points on planes a_1 and a_4 (Fig. 1)) at 1 d, 3 d, 5 d, 7 d, 9 d, 11 d, 13 d, 15 d, and 17 d of fermentation (a total of 90 vinegar Pei samples), respectively. All the

operational procedures, including DNA extraction, amplification, library construction, sequencing, and data analysis, were performed by Biomarker Technologies Co. (Beijing, China). To determine the bacterial community, the bacterial 16S rDNA genes were amplified using the 27F (5′-AGRGTTYGATYMTGGCTCAG-3′) forward primer and the 1492R (5′-RGYTACCTTGTTACGACTT-3′) reverse primer (Wang et al., 2021). To ascertain the fungal community, the ITS region was amplified using the ITS1F (5’-CTTGGTCATTTAGAGGAAGTAA-3') and ITS4 (5’-TCCTCCGCTTATTGATATG-C-3') primers (Shi et al., 2021). The reads were clustered into operational taxonomic units (OTUs) at 97% similarity using Usearch (version 10.0, www.drive5.com/uclust/). The alpha-diversity and beta-diversity were determined using BMKCloud (www.biocloud.net).

2.7 Statistical analysis

Kruskal-Wallis one-way analysis of variance by ranks and one-way analysis of variance with posthoc comparisons (Bonferroni tests) were conducted in IBM SPSS v21.0 (IBM, Armonk, NY, USA). The mycotoxin distribution in the fermentation basin was visualized using MATLAB R2017a (MathWorks, Natick, Massachusetts, USA).

3 Results and discussion

3.1 The spatial-temporal mycotoxin distribution during AAF vinegar processing

3.1.1 The mycotoxin content in the raw materials

DON, AFB_1, and ZEN represent the most prevalent mycotoxins in solid-state

fermentation substrates such as cereal chaff (Streit et al., 2013; Yu et al., 2019). In addition, Maiqu, the main enzyme donor during traditional vinegar fermentation, presents a mycotoxin contamination risk due to the aflatoxins and OTA in Daqu, a Baijiu fermentation starter (Zhang, et al., 2021). The main ingredient of Daqu is raw wheat, supplemented by a percentage of barley and peas, while Maiqu is produced via wheat crushing, water addition, mixing, pressing, forming, and cultivation at a certain temperature and humidity (Du et al., 2022).

As shown in Table S1, DON, AFB_1, and ZEN were identified in the raw materials used to produce the vinegar. The DON and ZEN levels in the wheat bran were higher than in the rice husk and Maiqu. Contrarily, the Maiqu presented the highest AFB_1 content compared with the wheat bran and rice husk. However, the levels of the three mycotoxins in the final vinegar products were significantly lower than in the vinegar Pei and considerably lower than the maximum levels for mycotoxins in food (GB2761-2017, 2017). This may be attributed to dilution during the vinegar drenching process, where the vinegar Pei was rinsed with water after AAF.

3.1.2 The spatial-temporal DON distribution during AAF

The DON level in the sampling region during different solid-fermentation days is shown in Fig. 2A. During the middle and final AAF stages (7 d to 17 d), the DON content was significantly lower than in the early stage (1 d and 5 d). Moreover, the DON content showed distinct fluctuation during the early and middle stages, initially

decreasing from 490.51 ± 128.81 μg/kg at 1 d to 397.77 ± 64.26 μg/kg at 3 d (P = 0.017), followed by an increase to 454.15 ± 73.22 μg/kg (P = 0.013) at 5 d, and a significant decline to 373.46 ± 34.65 μg/kg (P < 0.001) at 7 d, where it remained constant until the end of fermentation. The significant DON content increase at 5 d may be attributed to the specific traditional process involving a second addition of wheat bran to the vinegar Pei. Furthermore, the DON distribution in each sampling plane showed that the high value (DON content > 700 μg/kg) areas were primarily limited to 1 d and 5 d, exhibiting relatively uniform dispersion on most planes during the 7 d to 17 d period (Fig. 2B).

The DON levels of the different sampling planes were compared to examine spatial distribution characteristics in the fermentation basin. In the x-axis direction, the heterogeneous DON content distribution was largely evident between 11 d and 15 d, with low levels on plane a_1 on some days during the AAF process (plane a_1 versus plane a_2 P = 0.001 and a_4 P = 0.001 at 11 d, plane a_1 versus plane a_4 P = 0.031 at 13 d, and plane a_1 versus plane a_2 P = 0.012 at 15 d (Fig. 2C)). As shown in Fig. 2D, significant differences were observed between the DON levels on the different planes in the y-axis direction throughout AAF. The DON content was significantly lower on plane c_1 than on planes c_2 and c_3 in the z-axis direction from 3 d to 5 d (plane c_1 versus plane c_2 P = 0.003 and plane c_3 P = 0.0002 at 3 d, while plane c_1 versus plane c_2 P = 0.009 and plane c_3 P = 0.001 at 5 d (Fig. 2E)).

3.1.3 The spatial-temporal AFB_1 distribution during AAF

The AFB_1 content of the sample points distributed in the vinegar Pei sampling region on different fermentation days is shown in Fig. 3A. The AFB_1 content was lower in the early fermentation stage than during the middle and final stages. From 1 d to 7 d, the AFB_1 content increased significantly from 0.24 ± 0.06 μg/kg to 0.48 ± 0.09 μg/kg ($P < 0.001$). Although no obvious differences were evident between the AFB_1 levels on the different fermentation days during the middle and final AAF stages, considerable spatial heterogeneity was observed on some planes, such as plane c_3 at 7 d and 17 d (Fig. 3B).

Furthermore, the spatial AFB_1 heterogeneity was largely limited to the cross-sectional planes between 3 d and 11 d (Fig. 3C). A high AFB_1 level was detected on plane a_3, especially at 9 d (plane a_3 versus plane a_1 $P < 0.001$, plane a_2 $P < 0.001$, and plane a_4 $P = 0.049$) and 11 d (plane a_3 versus plane a_1 $P = 0.009$, plane a_2 $P = 0.012$, and plane a_4 $P = 0.038$). No significant AFB_1 content differences were evident between the different planes in the y-axis and z-axis directions on most fermentation days (Fig. 3D and Fig. 3E).

3.1.4 The space-time ZEN distribution during AAF

Fig. 4A shows the ZEN levels at the sample points distributed in the sampling region of the vinegar Pei on different fermentation days, which were significantly lower during the early and middle fermentation stages than in the final stage (n = 36 in the vinegar Pei samples throughout fermentation). In addition, the ZEN content changed significantly between 7 d and 11 d, increasing substantially from 25.48 ±

291 4.87 μg/kg to 36.67 ± 7.57 μg/kg ($P < 0.001$), followed by a considerable rise to 46.27
292 ± 6.28 μg/kg ($P < 0.001$). Although no significant differences were apparent between
293 the ZEN levels during the 11 d to 17 d period, the spatial ZEN distribution map of
294 each plane showed strong spatial heterogeneity (Fig. 4B).

295 Moreover, the ZEN exhibited similar distribution characteristics to AFB_1 in the
296 fermentation basin. The significant differences between the ZEN levels on the
297 different planes were largely limited to the cross-sectional planes during the final
298 stage of fermentation (9 d, 13 d, and 15 d (Fig. 4C)) and were negligible in the y-axis
299 and z-axis directions on most fermentation days (Fig. 4D and Fig. 4E).

300 *3.1.5 A comparison between the DON, AFB_1, and ZEN distribution characteristics*

301 The AAF process significantly affected the content and distribution of the three
302 mycotoxins in the vinegar Pei, with the DON variation trend completely distinct from
303 AFB_1 and ZEN. The average DON level exhibited a 17.17% decrease at the end of
304 AAF compared with the first day, while the average AFB_1 and ZEN content increased
305 considerably to 141.67% and 113.64%, respectively.

306 In addition, the significant AFB_1 and ZEN content variation was largely limited
307 to the cross-sectional sampling planes, while DON was heterogeneously distributed
308 on the cross-sectional, horizontal, and vertical sampling planes during AAF.
309 Therefore, DON, AFB_1, and ZEN showed different spatial distribution patterns in the
310 AAF basin.

311 *3.2 The physicochemical parameter changes in the vinegar Pei during AAF and their*

impact on the mycotoxins

The moisture content showed a narrow fluctuation range from 66.53% to 69.91% (Table S2). The moisture gradually rose due to gravity as the vinegar Pei depth increased in the y-axis direction. The moisture level in the shallow vinegar Pei layer (plane b_1) ranged from 60.55-65.97% throughout the AAF process while remaining at about 67% in the middle layer (plane b_2) and varying between 72.72% and 77.05% in the deep layer (plane b_3). In addition, no significant differences were observed between the moisture levels in the x-axis and z-axis directions.

The pH changes in the vinegar Pei during the AAF process were consistent with a previous report by Duan, et al. (2019). During the 1 d to 9 d period, the pH value of the vinegar Pei was down-regulated from 4.86 ± 0.39 to 3.61 ± 0.03 and remained constant at around 3.60 until 13 d, after which it increased to 3.65 ± 0.02 at the end of AAF (Table S2). Moreover, heterogeneous pH distribution was observed in different directions during most of the AAF process.

The impact of the physicochemical parameters on the mycotoxins was analyzed. The pH value was negatively correlated with the AFB_1 ($r = -0.752$, $P < 0.001$) and ZEN content ($r = -0.558$, $P < 0.001$) and positively associated with the DON level ($r = 0.409$, $P < 0.001$). In contrast, the influence of the moisture content on the mycotoxins was negligible.

3.3 The microbial community compositions in the vinegar Pei during AAF

The vinegar Pei samples from the 10 sampling sites (sites 1-5 represented

sampling points 2, 4, 5, 6, and 8 on plane a_1, and sites 6-10 denoted sampling points 2, 4, 5, 6, and 8 on a_4 (Fig. 1)) and the raw fermentation materials were investigated via amplicon sequencing analysis. A total of 60 OTUs were scattered in 42 genera in the collected samples throughout the AAF process. The dominant OTUs with an average relative abundance exceeding 5% were assigned to *Lactobacillus helveticus and Lactobacillus acetotolerans* (annotated as OTU1 and OTU2)*, Acetilactobacillus jinshanensis* (OTU3), and *Acetobacter pasteurianus* (OTU4), which accounted for 62.64-99.96% of the total abundance during the AAF process. Principal co-ordinates analysis (PCoA) (Fig. 5A) showed that the bacterial communities during AAF were further divided into three groups, which was consistent with the three AAF processing stages. The bacterial community succession during fermentation was generally consistent with previous reports (Wang, et al., 2016).

OTU1 and OTU2 dominated during the early AAF stage (1 d to 5 d) (Fig. 5B) since *Lactobacillus* was tolerant to ethanol, which was introduced via the fermented rice mash. As shown in Fig. S4 and Fig. S5, the bacterial communities in the vinegar Pei at 1 d exhibited the highest diversity during AAF. In addition to OTU1, bacterial OTU5 (*Cenchrus americanus*) was mainly produced by the wheat bran, while OTU7 (*Rhizobium Larrymoorei ATCC 51759*) was derived from the rice husk and OTU3 from the vinegar seeds.

During the mid-stage of AAF (at 7 d), OTU2 and OTU3 were the dominant bacteria, while the relative abundance of OTU1 and OTU2 were downregulated.

354 Contrarily, the relative abundance of OTU3 and OTU4 increased markedly from 7 d
355 due to their tolerance to acetic acid, which also dominated during the 9 d to 17 d
356 period of AAF.

357 The fungal community composition in the vinegar Pei throughout the AAF
358 process could be further divided into two stages based on PCoA (Fig. 5C). OTU1
359 (*Alternaria destruens*) and OTU3 (*Fusarium aethiopicum*) were the dominant fungi
360 during the 1 d to 5 d period, with a maximal relative abundance of 55.47% and
361 25.88%, respectively, followed by a gradual decline (Fig. 5D). The fungal community
362 in the vinegar Pei at 1 d was mainly composed of OTU1, OTU3, and other fungal
363 OTUs with a relative abundance below 5%. OTU1 was produced primarily by the
364 wheat bran, while OTU3 was derived from the wheat bran and vinegar seeds. Other
365 OTUs, such as OTU11 (*unclassified Fungi*) and OTU22 (*Aspergillus penicillioides*),
366 were derived from the rice husk and Maiqu.

367 Furthermore, between 7 d and 11 d, *Aspergillus heterocaryoticus* (OTU2)
368 gradually became the dominant fungi, while the other abundant fungal OTUs were
369 represented by *Brettanomyces bruxellensis* (OTU7) with an average relative
370 abundance of around 12.60%. In addition, OTU2 and OTU5 (*Rasamsonia*
371 *composticola*) dominated during the 13 d to 17 d period, with a relative abundance
372 ranging from 32.68-45.53% and 24.72-27.15%, respectively.

373 However, the microbial community composition variation in the fermentation
374 basin was analyzed via unweighted pair-group analysis (UPGMA). As depicted in

Fig. 6, the bacterial and fungal communities in the vinegar Pei collected on different fermentation days were grouped into 2-4 major clusters. Moreover, the microbial community compositions across the adjacent sampling area were distinct, and the composition in each cluster displayed successive variations with the progression of AAF. This suggests that the characteristics of the microbial community compositions in the fermentation basin correspond with the solid-state, stratified ZAV fermentation.

3.4 The correlation between the mycotoxins and microorganisms during the AAF process

Several studies have demonstrated that food processing (milling, roasting, and fermentation) affects the mycotoxin content in the final cereal-based products (Milani and Maleki, 2014; Khaneghah, et al., 2018). Therefore, increasing attention has been directed toward the potential impact of indigenous microbial communities on mycotoxins during the fermentation process (Adácsi, et al., 2022; Yang, et al., 2018). RDA (Fig. 5E) and CCA (Fig.5G) analysis revealed mycotoxin and bacterial correlations, especially regarding the abundant taxa (average relative abundance > 10% in at least one stage of AAF). *Lactobacillus helveticus* (OTU1) presented a positive correlation with the DON content (r = 0.279, P = 0.007) based on the Spearman correlation coefficients, while it was negatively correlated with AFB_1 and ZEN (r = −0.697, P < 0.0001 for AFB_1; r = −0.766, P < 0.0001 for ZEN (Fig. 5F)). *Lactobacillus acetotolerans* (OTU2) was negatively associated with the ZEN content (r = −0.359, P = 0.0005). *Acetobacter pasteurianus* (OTU4) showed a significantly

396 negative correlation with the DON content (r = −0.238, P = 0.024), while it was
397 positively associated with AFB_1 (r = 0.512, P < 0.0001) and ZEN (r = 0.743, P <
398 0.0001). Besides, positive correlations were evident between *Acetilactobacillus*
399 *jinshanensis* (OTU3) and AFB_1 (r = 0.632, P < 0.0001) and ZEN (r = 0.478, P <
400 0.0001). Although previous studies have indicated that AFB_1 and ZEN can be
401 degraded by *Acetobacter* and *Lactobacillus* (e.g., *Lactobacillus helveticus*) (Byun and
402 Yoon, 2003; Huang, et al., 2018), minimal research is available regarding the effect of
403 *Acetilactobacillus* on mycotoxin level.

404 Regarding the relationship between the fungal community and the three
405 mycotoxins, *Aspergillus heterocaryoticus* (OTU2) and *Rasamsonia composticola*
406 (OTU5) displayed significant positive correlations with AFB_1 (r = 0.561, P < 0.0001;
407 r = 0.439, P < 0.0001, respectively) and ZEN (r = 0.560, P < 0.0001; r = 0.653, P <
408 0.0001, respectively) (Fig. 5F), while *Alternaria destruens* (OTU1) and *Fusarium*
409 *aethiopicum* (OTU3) were negatively correlated with AFB_1 (r = −0.579, P < 0.0001; r
410 = −0.652, P < 0.0001, respectively) and ZEN (r = −0.738, P < 0.0001; r = −0.764, P <
411 0.0001, respectively). Although previous studies confirmed that ZEN and DON were
412 produced by *Fusarium* (e.g., *Fusarium graminearum*) (Dogi, et al., 2013; Hassan and
413 Bullerman, 2008), literature regarding the impact of *Alternaria destruens* and
414 *Fusarium aethiopicum* on mycotoxins remain insufficient. Therefore, the impact of
415 specific bacterial and fungi species from vinegar Pei on mycotoxins needs additional
416 evaluation.

4 Conclusions

This study investigates the spatial-temporal mycotoxin distribution in a solid-state fermentation basin during traditional vinegar processing and its potential correlation with microorganisms. The average DON content fluctuates from 1 d to 7 d, while the average AFB_1 and ZEN levels increase significantly during the 5 d to 7 d and 7 d to 11 d fermentation periods, respectively. The DON, AFB_1, and ZEN levels remain stable between 11 d and 17 d. However, the significant AFB_1 and ZEN content differences are largely limited to the cross-sectional planes in the fermentation basin, while DON is heterogeneously distributed on the cross-sectional, horizontal, and vertical planes throughout the AAF process. Based on the Spearman correlation coefficients, associations are identified between the predominant microbial populations and the mycotoxins, indicating the presence of some microorganisms with mycotoxin elimination capabilities. The results of this study bridge the gap between the spatial-temporal mycotoxin distribution and traditional Chinese vinegar production to improve the manufacturing process and establish an early warning system.

However, the complicated impact of microorganisms on the mycotoxins in vinegar Pei and the potential interaction mechanism requires further exploration. Furthermore, the reason for the lower levels of the three mycotoxins in the final vinegar products as compared to vinegar Pei needs additional assessment.

Acknowledgment

This work was supported by the Key Research Development Program of Jiangsu Province and Zhenjiang City, China (BZ2022030; GJ202012; GJ2021011; GJ2022002).

References

Adacsi, C., Kovacs, S., Pocsi, I., Gyori, Z., Dombradi, Z., & Pusztahelyi, T. (2022). Microbiologi cal and Toxicological Evaluation of Fermented Forages. *Agriculture-Basel*, *12*(3), 421. https:// doi.org/ 10.3390/agriculture12030421

Al-Dalali, S., Zheng, F. P., & Sun, B. G. (2023). Processing Technologies and Flavor Analysis of Chinese Cereal Vinegar: a Comprehensive Review. *Food Analytical Methods*, *16*(1), 1-28. https:// doi.org/10.1007/s12161-022-02328-w

Awuchi, C. G., Ondari, E. N., Nwozo, S., Odongo, G. A., Eseoghene, I. J., Twinomuhwezi, H., Ogbonna, C. U., Upadhyay, A. K., Adeleye, A. O., & Okpala, C. O. R. (2022). Mycotoxins' toxicological mechanisms involving humans, livestock and their associated health concerns: A review. *Toxins*, *14*(3), 33. https://doi.org/10.3390/toxins14030167

Byun, J. R., & Yoon, Y. H. (2003). Binding of aflatoxin G(1), G(2) and B-2 by probiotic Lactobacillus spp. *Asian-Australasian Journal of Animal Sciences*, *16*(11), 1686-1689. https://doi.org/10.5713/ajas.2003.1686

Chien, M.Y., Yang, C.M., Huang, C.M., & Chen, C.H. (2018). Investigation of aflatoxins conta mination in herbal materia medica in a Taiwan pharmaceutical factory. *Journal of Food and Drug Analysis*, *26*(3), 1154-1159. https://doi.org/10.1016/j.jfda.2018.01.016

Di, Y. H., Li, J. H., Chen, J., Zhao, X. R., & Du, G. C. (2023). Simulation and Control of the Formation of Ethyl Carbamate during the Fermentation and Distillation Processes of Chinese Baijiu. *Foods*, *12*(4). https://doi.org/10.3390/foods12040821

Dogi, C. A., Fochesato, A., Armando, R., Pribull, B., de Souza, M. M. S., Coelho, I. D., de Melo, D. A., Dalcero, A., & Cavaglieri, L. (2013). Selection of lactic acid bacteria to promote an efficient silage fermentation capable of inhibiting the activity of Aspergillus parasiticus and Fusarium gramineraum and mycotoxin production. *Journal of Applied Microbiology*, *114*(6), 1650-1660. https://doi.org/10.1111/jam.12173

Du, Z., Shan, Z., Shen, C., Cheng, F., Guo, H., Zang, W., Sun, J., Pan, X. (2022). Community structure and diversity formation of fermentation fungi in traditional Shaoxing Huangjiu. *Chinese Journal of Applied Ecology, 33*(4), 1118-1124. https://doi.org/10.13287/j.1001-9332.202204.040

Duan, W., Xia, T., Zhang, B., Li, S., Zhang, C., Zhao, C., Song, J., & Wang, M. (2019). Changes of Physicochemical, Bioactive Compounds and Antioxidant Capacity during the Brewing Process of Zhenjiang Aromatic Vinegar. *Molecules*, *24*(21). https://doi.org/10.3390/molec ules24213935

Ekwomadu, T. I., Akinola, S. A., & Mwanza, M. (2021). Fusarium Mycotoxins, Their Metabolites (Free, Emerging, and Masked), Food Safety Concerns, and Health Impacts. *International Journal of Environmental Research and Public Health*, *18*(22). https://doi.org/10.3390/ijerph 182211741

GB2761-2017, 2017. China national standard: Hygienic standard for grain. Beijing: Chinese standard publishing house.

Gong, M., Zhou, Z., Liu, S., Zhu, S., Li, G., Zhong, F., & Mao, J. (2021). Dynamic changes in physico-chemical attributes and volatile compounds during fermentation of Zhenjiang vinegars made with glutinous and non-glutinous japonica rice. *Journal of Cereal Science,*

100, 7. https://doi.org/10.1016/j.jcs.2021.103246

Hassan, Y. I., & Bullerman, L. (2008). Antifungal Activity of Lactobacillus paracasei subsp tolerans against Fusarium proliferatum and Fusarium graminearum in a Liquid Culture Setting. *Journal of Food Protection*, *71*(11), 2213-2216. https://doi.org/10.4315/0362-028x-71.11.2213

Huang, T., Lu, Z.-M., Peng, M.-Y., Liu, Z.-F., Chai, L.-J., Zhang, X.-J., Shi, J.-S., Li, Q., & Xu, Z.-H. (2022). Combined effects of fermentation starters and environmental factors on the microbial community assembly and flavor formation of Zhenjiang aromatic vinegar. *Food Research International*, *152*, 110900. https://doi.org/10.1016/j.foodres.2021.110900

Huang, W., Chang, J., Wang, P., Liu, C., Yin, Q., Zhu, Q., Lu, F., & Gao, T. (2018). Effect of the combined compound probiotics with mycotoxin-degradation enzyme on detoxifying aflatoxin B-1 and zearalenone. *Journal of Toxicological Sciences*, *43*(4-6), 377-385. https://doi.org/10.2131/jts.43.377

Jeong, S. E., Chung, S. H., & Hong, S. Y. (2019). Natural occurrence of aflatoxins and ochratoxin A in meju and soybean paste produced in South Korea. *Applied Biological Chemistry*, *62*(1), 65. https://doi.org/10.1186/s13765-019-0472-y

Kong, W. J., Wei, R. W., Logrieco, A. F., Wei, J. H., Wen, J., Xiao, X. H., & Yang, M. H. (2014). Occurrence of toxigenic fungi and determination of mycotoxins by HPLC-FLD in functional foods and spices in China markets. *Food Chemistry*, *146*, 320-326. https://doi.org/10.1016/j.foodchem.2013.09.005

Li, S., Li, C., Chen, S., Wang, X., Liu, J., Deng, X., Cai, H., & Liu, G. (2023). Effects of Solid-State Fermentation on the Standardized Ileal Digestibility of Amino Acids and Apparent Metabolizable Energy in Peanut Meal Fed to Broiler Chickens. *Fermentation-Basel*, *9*(4), 346. https://doi.org/10.3390/fermentation9040346

Li, H., Huang, W., Yi, B., Yang, J., & Yang, P. (2012). Ethanol/Moisture Contents in Fermented Grains and their Effects on the Yield and Quality of Chinese Luzhou-flavor Liquor. *Advances in Chemical Engineering*, *396-398*, 1605-1610. https://doi.org/10.4028/www.scientific.net/AMR.396-398.1605

Liu, Z., Zhang, X., Duan, X., Kang, B., Liu, J., Fu, C., Wang, C., Li, D., & Xu, N. (2022(1)). Effect of fermentation conditions on the formation of ammonium salt in soy sauce. *Lwt-Food Science and Technology*, *153*, 7. https://doi.org/10.1016/j.lwt.2021.112492

Liu, L. B., Chen, X. Q., Hao, L. L., Zhang, G. F., Jin, Z., Li, C., Yang, Y. Z., Rao, J. J., & Chen, B. C. (2022(2)). Traditional fermented soybean products: processing, flavor formation, nutritional and biological activities. *Critical Reviews in Food Science and Nutrition*, *62*(7), 1971-1989. https://doi.org/10.1080/10408398.2020.1848792

Lu, Y. H., Yang, L. Z., Yang, G. H., Chi, Y. L., Sun, Q., & He, Q. (2021). Insight into the Fermentation of Chinese Horse Bean-chili-paste. *Food Reviews International*, *37*(7), 683-705. https:// doi.org/10.1080/87559129.2020.1717525

Lu, Z. M., Wang, Z. M., Zhang, X. J., Mao, J., Shi, J. S., & Xu, Z. H. (2018). Microbial ecology of cereal vinegar fermentation: insights for driving the ecosystem function. *Current Opinion in Biotechnology*, *49*, 88-93. https://doi.org/10.1016/j.copbio.2017.07.006

Milani, J., & Maleki, G. (2014). Effects of processing on mycotoxin stability in cereals. *Journal of*

The Science of Food and Agriculture, *94*(12), 2372-2375. https://doi.org/10.1002/jsfa.6600

Khaneghah, A. M., Fakhri, Y., & Sant'Ana, A. S. (2018). Impact of unit operations during processing of cereal-based products on the levels of deoxynivalenol, total aflatoxin, ochratoxin A, and zearalenone: A systematic review and meta-analysis. *Food Chemistry*, *268*, 611-624. https://doi.org/10.1016/j.foodchem.2018.06.072

Shen, C. (2022). *China Food Industry Yearbook* (part 33). *Jilin Science and Technology Press* (Chapter 2).

Shen, Z., Yu, Y., Zhu, S., Yang, Y., & Wang, H. (2016). Research on key techniques of non-material cultural heritage of Zhenjiang vinegar brewing techniques. *China Condiment*, *41*(10), 140-145. https://doi:10.3969/j.issn.1000-9973.2016.10.031

Shi, X., Zhao, X., Ren, J., Dong, J., Zhang, H., Dong, Q., ... & Yu, H. (2021). Influence of peanut, sorghum, and soil salinity on microbial community composition in interspecific interaction zone. *Frontiers in Microbiology*, *12*, 678250. https://doi.org/10.3389/fmicb.2021.678250

Streit, E., Naehrer, K., Rodrigues, I., & Schatzmayr, G. (2013). Mycotoxin occurrence in feed and feed raw materials worldwide: long-term analysis with special focus on Europe and Asia. *Journal of The Science of Food and Agriculture*, *93*(12), 2892-2899. https://doi.org/10.1002/jsfa.6225

Sun, W. L., Shahrajabian, M. H., & Lin, M. (2022). Research Progress of Fermented Functional Foods and Protein Factory-Microbial Fermentation Technology. *Fermentation-Basel*, *8*(12), 688. https://doi.org/10.3390/fermentation8120688

Tu, W., Cao, X., Cheng, J., Li, L., Zhang, T., Wu, Q., Xiang, P., Shen, C., & Li, Q. (2022). Chinese Baijiu: The Perfect Works of Microorganisms. *Frontiers in Microbiology*, *13*, 20. https://doi.org/10.3389/fmicb.2022.919044

Wall-Martinez, H. A., Pascari, X., Bigorda, A., Ramos, A. J., Marin, S., & Sanchis, V. (2019). The fate of Fusarium mycotoxins (deoxynivalenol and zearalenone) through wort fermenting by Saccharomyces yeasts (S. cerevisiae and S. pastorianus). *Food Research International*, *126*, 108587. https:// doi.org/10.1016/j.foodres.2019.108587

Wall-Martinez, H. A., Pascari, X., Ramos, A. J., Marin, S., & Sanchis, V. (2020). Fate of the mycotoxins in the wort and yeast during ale and lager fermentation and their evaluation under different technological parameters. *Lwt-Food Science and Technology*, *132*, 109877. https://doi.org/10.1016/j.lwt.2020. 109877

Wang, H. Y., Zhang, C. X., Cheng, P., Wang, Y., Liu, H. M., Wang, H. F., Wang, H. W., & Gong, M. Q. (2021). Differences in the intestinal microbiota between insecticide-resistant and -sensitive Aedes albopictus based on full-length 16S rRNA sequencing. *Microbiologyopen*, *10*(2), e1177. https://doi.org/10.1002/mbo3.1177

Wang, Z.M., Lu, Z.M., Shi, J.S., & Xu, Z.H. (2016). Exploring flavour-producing core microbiota in multispecies solid-state fermentation of traditional Chinese vinegar. *Scientific Reports*, *6*, 26818. https://doi.org/10.1038/srep26818

Wang, Z.M., Lu, Z.M., Yu, Y.J., Li, G.Q., Shi, J.S., & Xu, Z.H. (2015). Batch-to-batch uniformity of bacterial community succession and flavor formation in the fermentation of Zhenjiang aromatic vinegar. *Food Microbiology*, *50*, 64-69. https://doi.org/10.1016/j.fm. 2015.03.012

Woo, S. Y., Ryu, S. Y., Tian, F., Lee, S. Y., Park, S. B., & Chun, H. S. (2019). Simultaneous

Determination of Twenty Mycotoxins in the Korean Soybean Paste Doenjang by LC-MS/MS with Immunoaffinity Cleanup. *Toxins*, *11*(10), 19. https://doi.org/10.3390/toxins11100594

Yang, L. J., Yang, Z. B., Yang, W. R., Li, H. R., Zhang, C. Y., Jiang, S. Z., & Li, X. M. (2018). Conventional solid fermentation alters mycotoxin contents and microbial diversity analyzed by high-throughput sequencing of a Fusarium mycotoxin-contaminated diet. *Canadian Journal of Animal Science*, *98*(2), 354-361. https://doi.org/10.1139/cjas-2017-0093

Yu, J. M., Mikiashvili, N., & Lian, C. L. (2019). Deoxynivalenol and ochratoxin A in North Carolina grown organic wheat grains. *Journal of Food Safety*, *39*(6), e12687. https://doi.org/10.1111/jfs.12687

Yu, Z., Ma, Y., Guan, Y. F., Zhu, Y. Y., Wang, K., Wang, Y. Q., Liu, P., Chen, J., & Yu, Y. J. (2022). Metagenomics of Virus Diversities in Solid-State Brewing Process of Traditional Chinese Vinegar. *Foods*, *11*(20), 3296. https://doi.org/10.3390/foods11203296

Zhang, S. Y., Liu, S., Zeng, W. W., Long, W. Y., Nie, Y., Xu, Y., Yang, F., & Wang, L. (2021). The Risk Monitoring of Aflatoxins and Ochratoxin A in Critical Control Point of Soy Sauce Aroma-Type Baijiu Production. *Toxins*, *13*(12)., 876. https://doi.org/10.3390/toxins13120876

Zhang, S., Wei, Y., & Wang, L. (2022). Problems and supervisory counter measures in the implementation of national food safety standards for soy sauce and vinegar. *Food and Fermentation Industries*, *48*(7), 319-324. https://doi.org/10.13995/j.cnki.11-1802/ts.030106

Zhu, W., Ren, C., Nie, Y., & Xu, Y. (2016). Quantification of ochratoxin A in Chinese liquors by a new solid-phase extraction clean-up combined with HPLC-FLD method. *Food Control*, *64*, 37-44. https://doi.org/10.1016/j.foodcont.2015.11.044

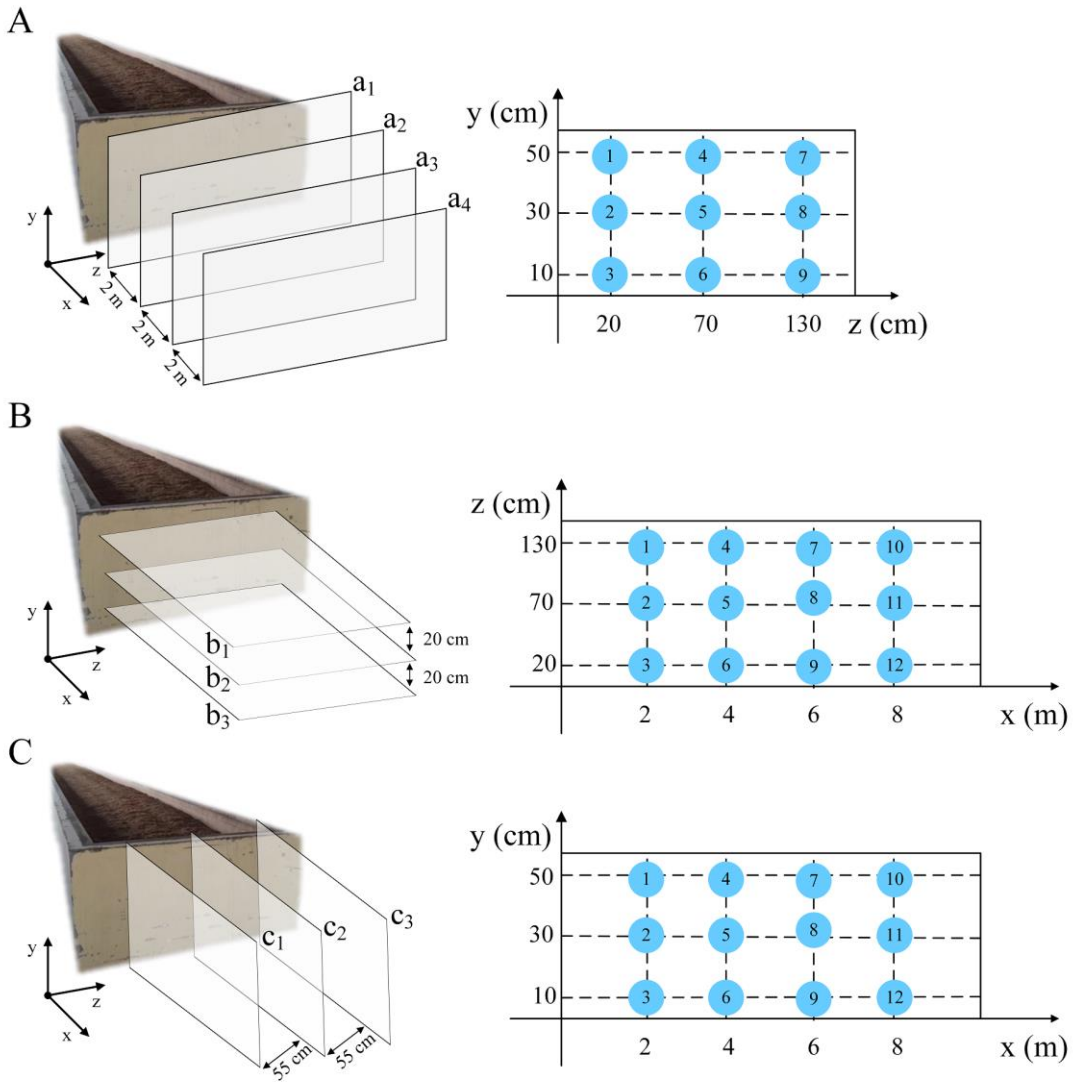

Fig. 1. The collection method of vinegar Pei in fermentation basin space. (A) The a_1, a_2, a_3 and a_4 are cross-sectional sampling planes divided in the x-axis direction, and there were 9 sampling points on each cross-sectional sampling plane. (B) The b_1, b_2, and b_3 are the horizontal sampling planes divided in the y-axis direction, and there were 12 sampling points on each horizontal sampling planes. (C) The c_1, c_2 and c_3 are the vertical sampling planes divided in the z-axis direction, and there were 12 sampling points on each vertical sampling planes.

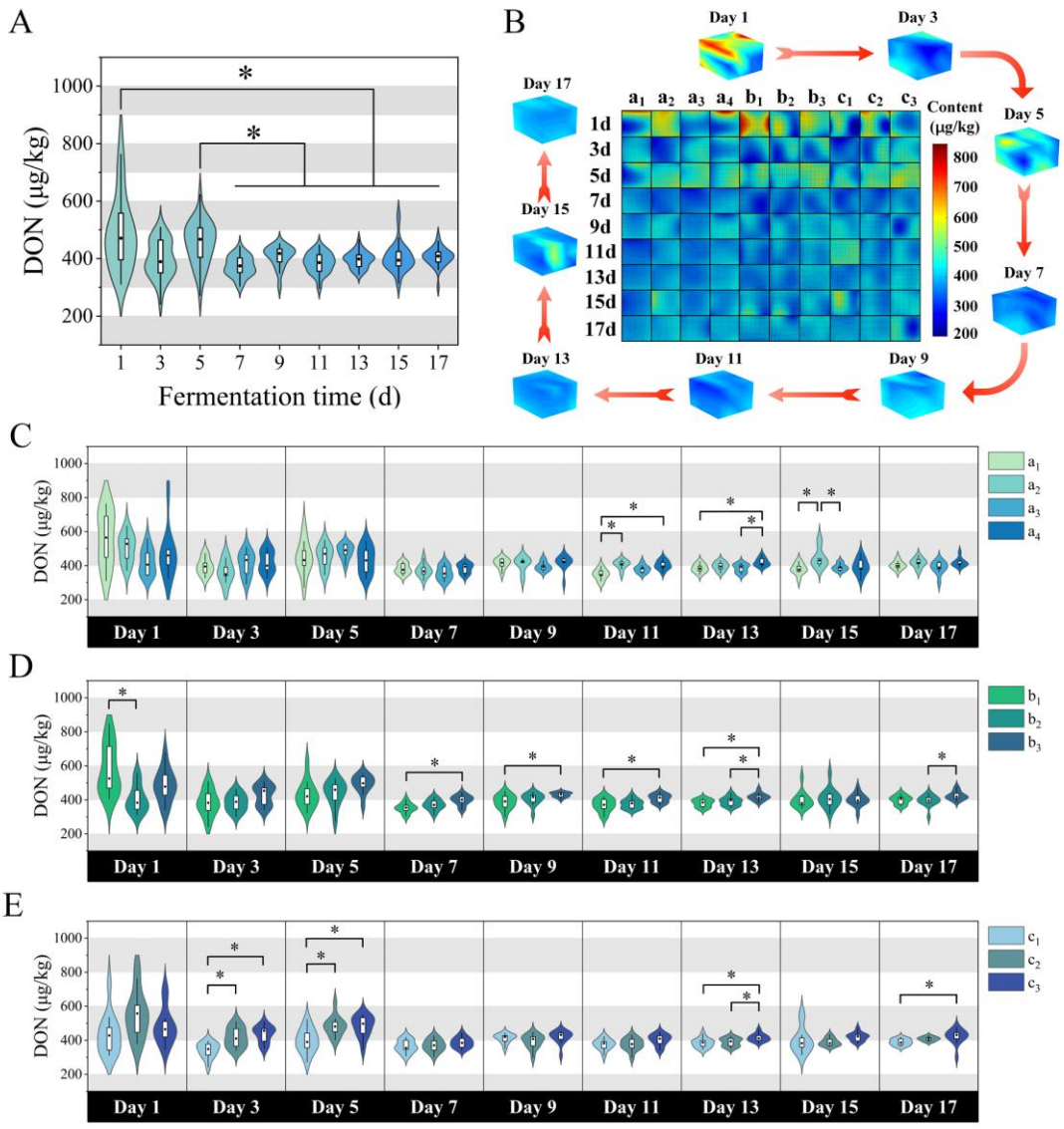

Fig. 2. The level and distribution of DON content in sampling region of the vinegar Pei. (A) The level of DON content in the sampling region during different solid-fermentation days (n = 36 in the vinegar Pei samples throughout the AAF process). (B) The DON distribution maps of fermentation basin surface and internal planes. The level and distribution of DON content on (C) cross-sectional planes, (D) horizontal plane and (E) vertical plane. In the violin plot, the black dot represents the middle; the white box edge showed the 25th and 75th percentiles and the whiskers extends to 1.5× the interquartile range. For A statistical analysis, Kruskal-Wallis one-way analysis of variance by ranks. For C-D statistical analysis, one-way analysis of variance with posthoc comparisons (Bonferroni tests).

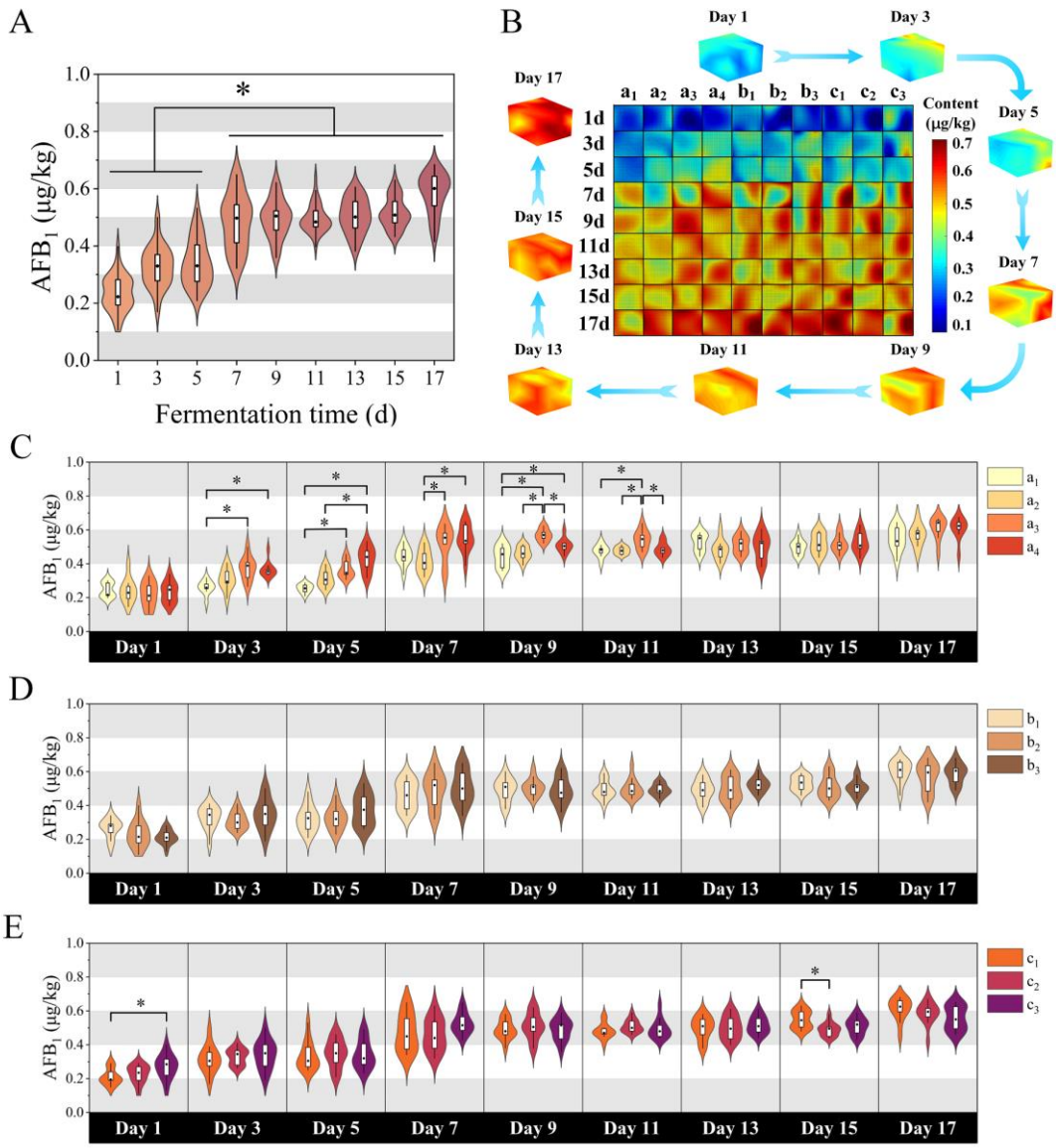

Fig. 3. The level and distribution of AFB_1 content in sampling region of the vinegar Pei. (A) The level of AFB_1 content in the sampling region during different solid-fermentation days (n = 36 in the vinegar Pei samples throughout the AAF process). (B) The AFB_1 distribution maps of fermentation basin surface and internal planes. The level and distribution of AFB_1 content on (C) cross-sectional planes, (D) horizontal plane and (E) vertical plane. In the violin plot, the black dot represents the middle; the white box edge showed the 25th and 75th percentiles and the whiskers extends to 1.5× the interquartile range. For A statistical analysis, Kruskal-Wallis one-way analysis of variance by ranks. For C-D statistical analysis, one-way analysis of variance with posthoc comparisons (Bonferroni tests).

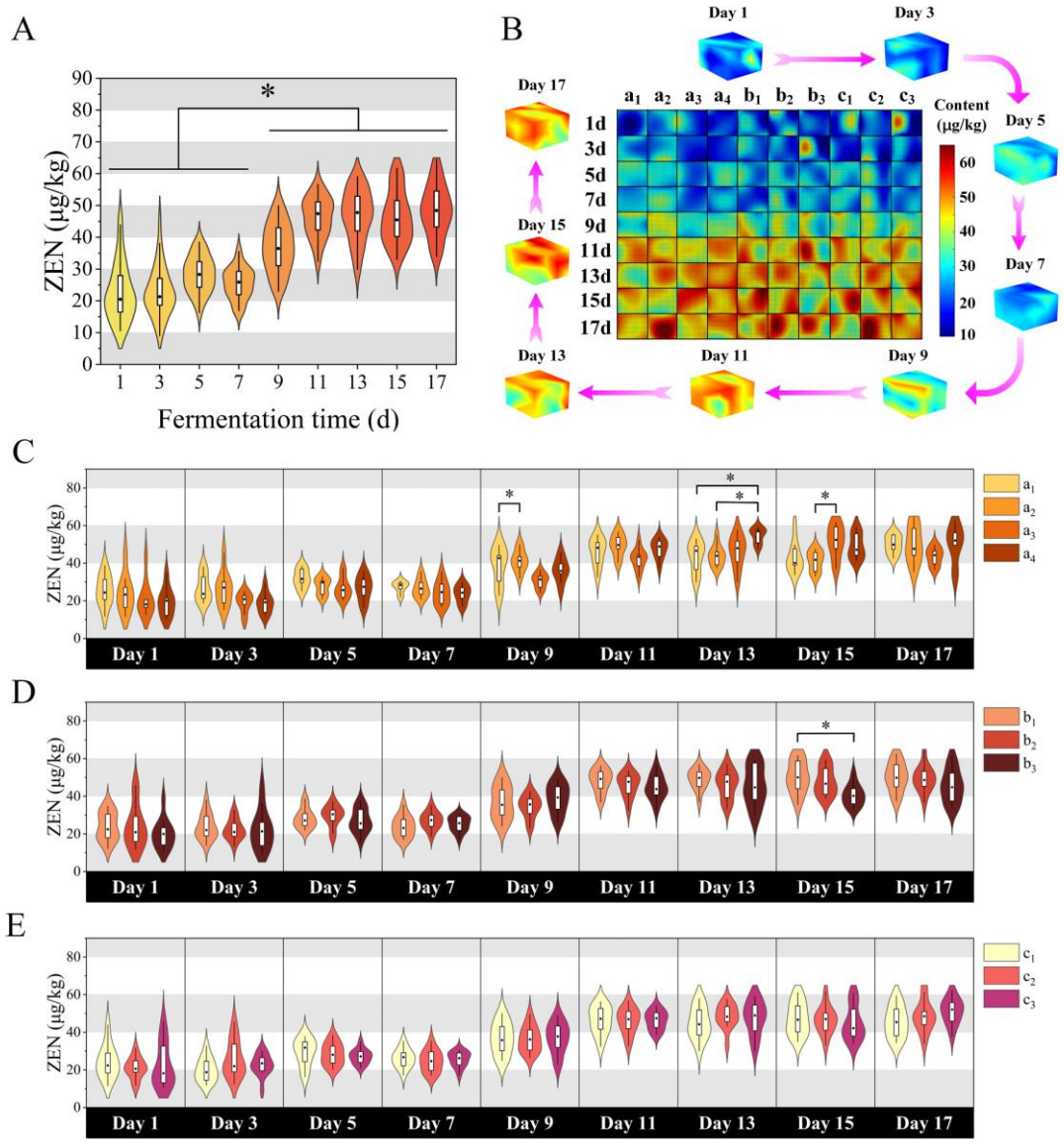

Fig. 4. The level and distribution of ZEN content in sampling region of the vinegar Pei. (A) The level of ZEN content in the sampling region during different solid-fermentation days (n = 36 in the vinegar Pei samples throughout the AAF process). (B) The ZEN distribution maps of fermentation basin surface and internal planes. The level and distribution of ZEN content on (C) cross-sectional planes, (D) horizontal plane and (E) vertical plane. In the violin plot, the black dot represents the middle; the white box edge showed the 25th and 75th percentiles and the whiskers extends to 1.5× the interquartile range. For A statistical analysis, Kruskal-Wallis one-way analysis of variance by ranks. For C-D statistical analysis, one-way analysis of variance with posthoc comparisons (Bonferroni tests).

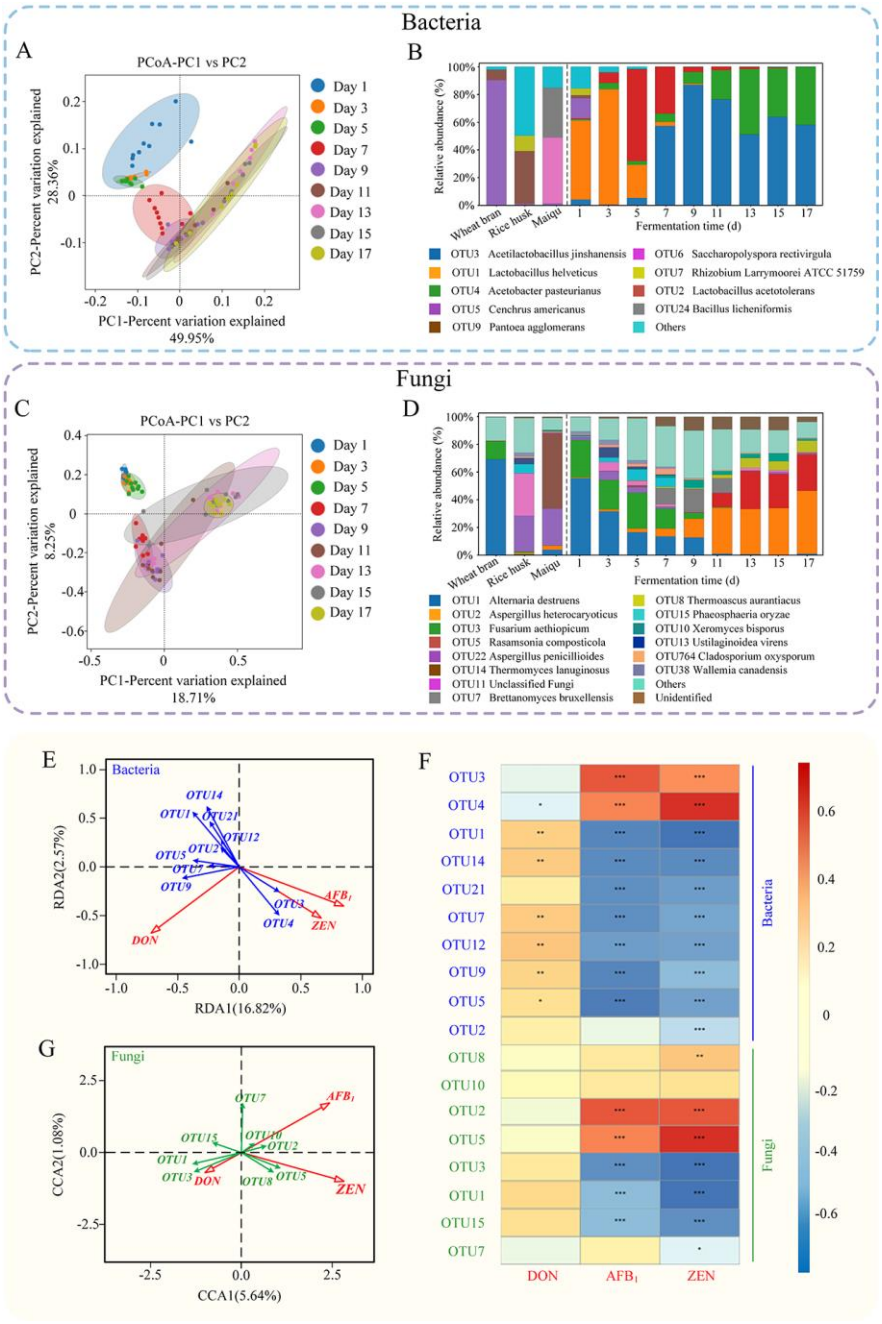

Fig. 5. Alternating patterns and correlation analysis of microbial communities during AAF. Principal coordinate analysis (PCoA) of the (A) bacterial and (C) fungal communities based on weighted Unifrac distances. Distribution of (B) bacterial and (D) fungal communities at the OTU level during the fermentation process. The OTUs with average relative abundance > 1%. (E) Correlation analysis by Redundancy analysis (RDA) between bacterial OTUs and mycotoxins during fermentation. (F) Spearman correlation coefficients of bacteria and fungi. *, $P < 0.05$; **, $P < 0.01$; ***, $P < 0.001$ (G) Correlation analysis by Canonical correspondence analysis (CCA) between fungal OTUs and mycotoxins during fermentation.

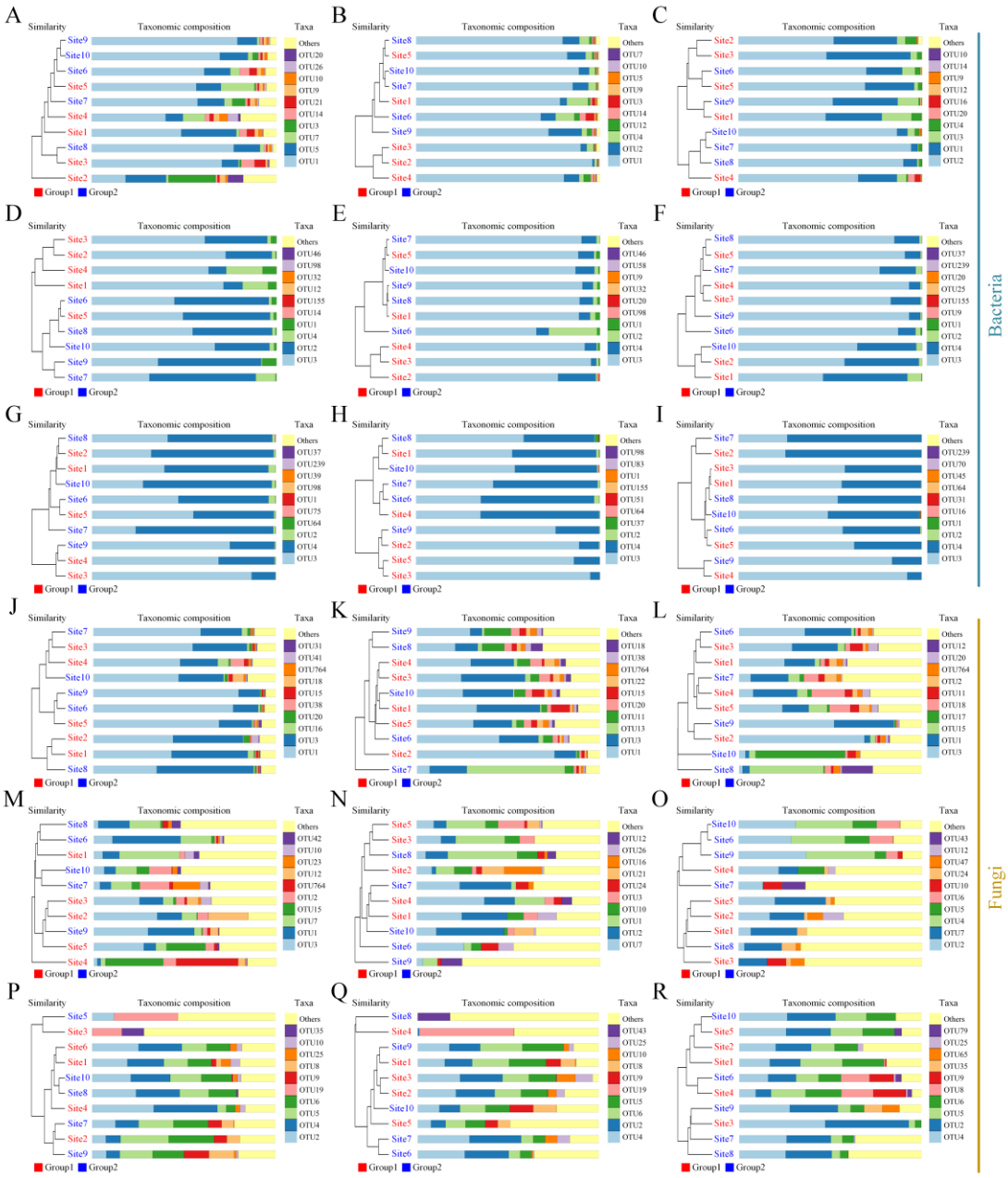

Fig. 6. Unweighted pair-group analysis (UPGMA) based on UniFrac distance for bacterial (A-I) and fungal (J-R) communities in 1 d, 3 d, 5 d, 7 d, 9 d, 11 d, 13 d, 15 d, and 17 d. Site 1-5 were sampling point 2, 4, 5, 6 and 8 on plane a1 and site 6-10 were sampling point 2, 4, 5, 6 and 8 on a_4.

Graphical abstract

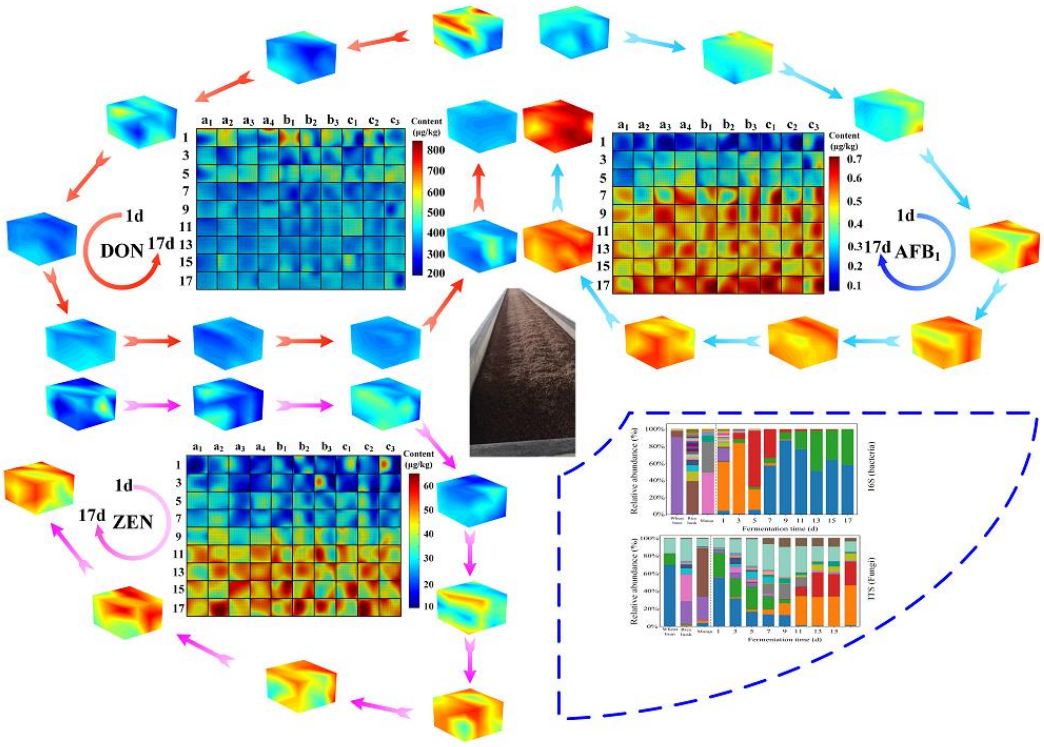

Credit author statement

Lingqin Shen: Conceptualization, Writing-Review & Editing, Project administration. **Yifan Wang**: Writing-original draft, Data Curation, Methodology. **Xin Li**: Resources, Formal analysis, Investigation. **Ziqing Hou**: Conceptualization. **Jin Mao**: Software and HPLC analysis. **Jiyong Shi**: Data curation. **Maurizio Battino**: Validation, Resources. **Michael N. Routledge**: Writing-Review & Editing. **Yunyun Gong**: Formal analysis. **Xiaobo Zou**: Project administration, Funding acquisition. **Di Zhang**: Supervision, Methodology, Investigation.

Conflicts of interest

The authors declare no conflict of interest.